Available online at www.sciencedirect.com

SCIENCE DIRECT

Developmental Biology 285 (2005) 57 – 69

DEVELOPMENTAL BIOLOGY

www.elsevier.com/locate/ydbio

The mouse *t* complex distorter/sterility candidate, *Dnahc8*, expresses a γ-type axonemal dynein heavy chain isoform confined to the principal piece of the sperm tail

Sadhana A. Samant[1], Olugbemiga O. Ogunkua[2], Ling Hui[3], Jing Lu, Yibing Han, Joanne M. Orth, Stephen H. Pilder*

Department of Anatomy and Cell Biology, Temple University School of Medicine, 3400 N. Broad Street, Philadelphia, PA 19140, USA

Received for publication 24 November 2004, revised 26 May 2005, accepted 3 June 2005
Available online 28 July 2005

Abstract

Heterozygosity for a *t* haplotype (*t*) in male mice results in distorted transmission (TRD) of the *t*-bearing chromosome 17 homolog to their offspring. However, homozygosity for *t* causes male sterility, thus limiting the spread of *t* through the population at large. The Ca^{2+}-dependent sperm tail curvature phenotypes, "fishhook", where abnormally high levels of sperm exhibit sharp bends in the midpiece, and "curlicue", where motile sperm exhibit a chronic negative curving of the entire tail, have been tightly linked to *t*-associated male TRD and sterility traits, respectively. Genetic studies have indicated that homozygosity for the *t* allele of *Dnahc8*, an axonemal γ-type dynein heavy chain (γDHC) gene, is partially responsible for expression of "curlicue"; however, its involvement in "fishhook"/TRD, if any, is unknown. Here we report that the major isoform of DNAHC8 is copiously expressed, carries an extended N-terminus and full-length C-terminus, and is stable and equally abundant in both testis and sperm from +/+ and *t/t* animals. By in silico analysis we also demonstrate that at least three of the seventeen $DNAHC8^t$ mutations at highly conserved positions in wild-type DHCs may be capable of substantially altering normal DNAHC8 function. Interestingly, DNAHC8 is confined to the principal piece of the sperm tail. The combined results of this study suggest possible mechanisms of $DNAHC8^t$ dysfunction and involvement in "curlicue", and support the hypothesis that "curlicue" is a multigenic phenomenon. They also demonstrate that the accelerated "fishhook" phenotype of sperm from +/*t* males is not directly linked to $DNAHC8^t$ dysfunction.

Keywords: *t* complex; Dynein heavy chain subtype; Inner dynein arm; Outer dynein arm; Axoneme; Flagellum; Flagellar waveform; Principal piece; Midpiece; Male sterility; Male TRD

Introduction

Mouse *t* haplotypes (*t*) are members of a closely related family of variant homologs of a 40 million base-pair region (the *t* complex) at the proximal end of chromosome 17, sharing four non-overlapping inversions (*In[17]1–In[17]4* from proximal to distal) relative to the wild-type (+) homolog (Lyon, 1984) (Fig. 1). Because these inversions cover approximately 95% of the *t* complex region, recombination between + and *t* is suppressed, with strong concomitant effects on the evolution and transmission of genes both within and immediately flanking the region (Hammer et al., 1989; Bartolome and Maside, 2004).

Both +/*t* males and females are fertile; however, +/*t* males exhibit transmission ratio distortion (TRD) in favor of *t*, so that >90% of their offspring receive the *t* homolog from their sire (Lyon, 1984). Genetic models suggest that

* Corresponding author. Fax: +1 215 707 2966.
E-mail address: stephen.pilder@temple.edu (S.H. Pilder).
[1] Present Address: Department of Medicine, Division of Biological Sciences, University of Chicago, Chicago, IL 60637, USA.
[2] Present Address: Department of Pathology, Anatomy, and Cell Biology, Meharry Medical College, Nashville, TN 37208, USA.
[3] Present Address: Department of OBGYN, University of Pennsylvania Medical Center, Philadelphia, PA 19104, USA.

0012-1606/$ - see front matter © 2005 Elsevier Inc. All rights reserved.
doi:10.1016/j.ydbio.2005.06.002

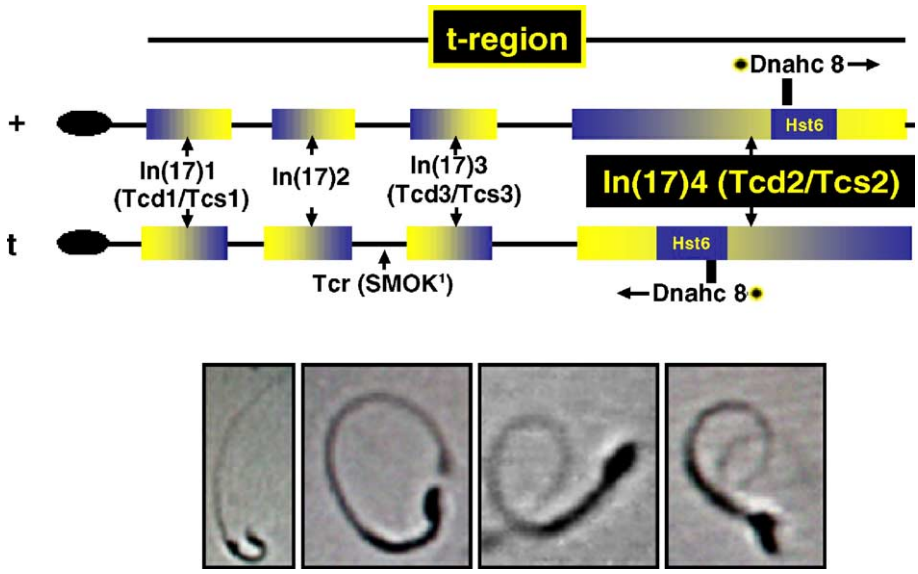

Fig. 1. (Top) The wild-type (+) and *t* haplotype (*t*) homologs of the mouse *t* complex. Homologous but inverted sequences are represented by horizontal lines with four differentially shaded rectangles superimposed upon each line. The filled ellipse on the left end of each homolog represents the centromere, the rectangles, labeled *In(17)1-In(17)4* between the homologs correspond to +-*t* relative inversions, and the inversions to which each distorter/sterility factor is located (*Tcd1/Tcs1*, *Tcd3/Tcs3*, and *Tcd2/Tcs2* from proximal to distal) are indicated, as is the position of the *t* responder/SPERM MOTILITY KINASE gene (*Tcr/SMOK*^{t}). The position of *Dnahc8* alleles in each distal-most inversion is indicated within the *Hybrid Sterility 6* (*Hst6*) locus. (Bottom) Digital photographs captured directly from videotapes of swimming sperm. From left to right, the panels show a wild-type sperm undergoing high Ca^{2+}-induced arrest. Note the "fishhook" curvature of the midpiece is also indicative of hyperactivated wild-type sperm as well as a high percentage of sperm from +/*t* animals, known to prematurely hyperactivate; and sperm from *t/t* males displaying the "curlicue" phenotype after approximately 15, 18, and 20 min in IVF medium, respectively. Note exaggerated negative curvature of the principal piece of the flagella of "curlicue" sperm relative to the wild-type arrested sperm.

TRD is the product of the expression of at least three *t* complex distorters (*tcds*) acting additively on a *t* complex responder (*tcr*; Fig. 1) (Lyon, 1984). While all *tcds* are capable of raising the transmission ratio of the homolog carrying *tcr*, *tcd2*, the distorter factor located in the large *In(17)4* clearly has the strongest effect on *t* transmission (Lyon, 1984, 2003). Interestingly, male TRD in favor of *t* is offset by the absolute sterility of *t/t* males.

Because *t*-associated male sterility localized to the inversions carrying the *tcds*, and the strength of each sterility factor exhibited a strength directly proportional to the strength of the *tcd* mapping to the same inversion, Lyon (1986) posited the formal argument that homozygosity for *tcds* was responsible for the male sterility phenotype. This hypothesis, which implied that the causes of both aberrant phenotypes were closely related at the biochemical level, was reinforced by evidence that attributed both +/*t* TRD and *t/t* male sterility to aberrant sperm motility phenotypes related to flagellar curvature defects (Olds-Clarke and Johnson, 1993). However, recent studies have disputed the claim that *tcd1* in *In(17)1* is identical to the *t* complex sterility factor (*tcs1*) in that inversion (Schimenti et al., 2005), although *tcd2* has not yet been separated from the *t* complex sterility factor (*tcs2*) in *In(17)4*.

The molecular bases of +/*t* TRD and *t/t* male sterility are incompletely known. Nevertheless, the underlying pathophysiology of poor motility exhibited by sperm from males of *t*-bearing genotypes is better understood. Olds-Clarke and Johnson (1993) compared the motility of sperm produced by +/+, +/*t*, and *t/t* males. Their experiments revealed that when cauda epididymal sperm from +/+ males were released into a Ca^{2+}-containing medium that supports fertilization in vitro (IVF medium), they initially swam progressively with symmetrical flagellar bends. Approximately 30% of these sperm changed from progressive swimming to hyperactivated (vigorous but non-progressive) movement, a trait that normally occurs near the site of fertilization in vivo and is obligatory for successful fertilization (Ho and Suarez, 2003; Marquez and Suarez, 2004; Carlson et al., 2003). However, this change was gradual, requiring a 2-h incubation. Hyperactivated sperm also exhibited chronic negative curvature of the flagellar midpiece ("fishhook" phenotype), but similar curvature rarely occurred in the principal piece. In other studies, if the axonemal Ca^{2+} concentration was increased above a critical level for a lengthy period of time, wild-type sperm tails would arrest at one extreme of the beat cycle (Lindemann and Kanous, 1997; Schmitz-Lesich and Lindemann, 2004). The arrested flagella were generally characterized by the same chronic, negative curvature or "fishhook"-like appearance with maximal bending in the flagellar midpiece (Fig. 1). Thus, "fishhook" appeared to be a normal flagellar response to increased levels of Ca^{2+} in the medium.

The behavior of +/*t* and *t/t* sperm released into IVF medium was in stark contrast to the activity of sperm from +/+ males. In sperm from +/*t* males, abnormally high levels of sperm (60%) hyperactivated within 1 h, and hyperactivated sperm exhibited the "fishhook" trait. These

"fishhook" tails persisted even during a gradual decline in sperm swimming speed. As was the case for wild-type sperm, the principal piece of the tail generally exhibited wild-type behavior, although lengthy incubation in IVF resulted in transient abnormal negative curvature in the principal pieces of a few sperm.

In the case of sperm from *t/t* males, hyperactivation was nearly immediate (occurring after only a 5-min incubation in over 50% of the motile sperm). Just as quickly, this phenotype gave way to a sharp decline in sperm swimming speed, with almost all sperm exhibiting a vestige of motility plus absence of a regular beat pattern accompanied by a persistent, negative bend of both the flagellar midpiece and principal piece ("curlicue" phenotype). This trait could best be described as an exaggerated form of Ca^{2+}-induced flagellar "arrest" (Fig. 1) (Lindemann and Kanous, 1997; Schmitz-Lesich and Lindemann, 2004; Olds-Clarke and Johnson, 1993; Pilder et al., 1993). Since both Ca^{2+}-induced hyperactivation and motility arrest are thought to be products of alterations in dynein-based force production (Schmitz-Lesich and Lindemann, 2004), it was not surprising that the primary agents of "curlicue" were mapped to a complex of testis-expressed genes located in a small central area of *In(17)4* (*Hst6*) which included *Dnahc8*, an axonemal dynein heavy chain (DHC) gene with testis-restricted expression and seventeen missense mutations in its *t* allele (Table 1) (Pilder et al., 1993; Redkar et al., 1998; Samant et al., 1999; Fossella et al., 2000; Samant et al., 2002).

Initial studies suggested that *Dnahc8* (*AF356520* = + allele, *AF356522* = *t* allele) and its potential translation products belonged to the family of γ-type DHCs (γDHCs) (Tanaka et al., 1995; Chapelin et al., 1997; Samant et al., 2002), components of the outer dynein arm (ODA), a force-producing motor complex of the axoneme that is invariant in its heavy chain composition in *Chlamydomonas* flagella (Lindemann and Kanous, 1997). These studies also suggested that *Dnahc8* expressed several testis-specific mRNA isoforms coding for two C-termini of different lengths and in at least two isoforms, a seemingly non-abundant, unusual N-terminus with absolutely no relationship to the N-termini of any other known dynein heavy chain (DHC) (Fossella et al., 2000; Samant et al., 2002). The proximal two-thirds to three quarters of this unique N-terminus appeared to consist of two large PEST motifs interlaced with sequences suggestive of roles in signaling and protein–protein interaction (Samant et al., 2002), but the C-terminal part of this N-terminus was not thoroughly characterized. Additionally, all *Dnahc8* mRNA isoforms accumulated exclusively in late meiotic spermatocytes, implying that their translation would have to occur prior to spermiogenesis (Samant et al., 2002), the post-division male germ cell process of morphological differentiation spanning two or more weeks in mammals. This result indicated that if DNAHC8 polypeptides were present in mature sperm tails, they would have to be quite stable.

To elucidate DNAHC8 function in the mammalian sperm tail, we have studied the expression and subcellular localization of allelic DNAHC8 isoforms and have analyzed the $DNAHC8^t$ mutations by comparative alignment with 96 wild-type orthologous and paralogous DHC sequences. Our results support a role for $DNAHC8^t$ in manifestation of the "curlicue" phenotype but demonstrate that $DNAHC8^t$ is not the cause of the accelerated manifestation of "fishhook" observed in a high percentage of motile sperm from *+/t* animals. This suggests that $DNAHC8^t$ may not be a primary agent of TRD.

Table 1
List of $DNAHC8^t$ mutations

Position	+-*t* Δ	Stem/Motor
127	G→R	+/–
128	I→L	+/–
424	R→C	+/–
813	T→R	+/–
963	D→N	+/–
982	T→A	+/–
1051	E→K	+/–
1291	K→E	+/–
1421	V→I	+/–
1437	N→S	+/–
1463	V→E	+/–
1566	A→G	+/–
1569	D→N	+/–
2224	V→A	–/+
3408	P→T	–/+
3893	I→V	–/+
4229	E→K	–/+

Materials and methods

Mice and genotyping

Mice used in this study were maintained in the colony of S. Pilder at Temple University School of Medicine in accordance with NIH regulations/guidelines and IACUC protocols. The complete *t* haplotypes, t^{w5} and t^{w32}, the wild-type chromosome 17 homolog, and the previously described recombinant chromosome 17 homologs with $Dnahc8^S$ alleles (Redkar et al., 1998; Samant et al., 1999, 2002; Fossella et al., 2000) were maintained on the C57BL/6 genetic background. All experimental animals were genotyped by RFLP analysis of Southern blotted mouse tail-tip DNA using a variety of previously described informative markers (Pilder et al., 1993; Redkar et al., 1998; Samant et al., 1999, 2002; Fossella et al., 2000).

Antisera preparation

Three mono-specific polyclonal antisera (AS1, AS2, and AS3) were raised in rabbits against KLH-linked peptides from the longest potential mouse DNAHC8 isoform (GenBank accession no. AF356520) (Invitrogen, Carlsbad,

CA). Each peptide was selected on the basis of its computationally determined antigenicity, its location in the polypeptide, and its potential lack of cross-reactivity with other mouse proteins (see Results section for positions of peptides in the longest DNAHC8 isoform against which the antisera were raised). After ELISA analysis, each crude antiserum was affinity purified on a column of Sepharose-4B coupled to the peptide against which it was raised, followed by OD_{280} reading. Antiserum against human β-tubulin (H-235) was purchased from Santa Cruz Biotechnology (Santa Cruz, CA).

Dnahc8 5′-end analysis

Plaque lifts of previously described testis cDNA libraries (Samant et al., 2002) were screened with a probe consisting of exons 5, 6, and 7 of the full-length isoform of *Dnahc8*. Lifts were processed as previously described. Each 5′-end was isolated from independent clones at least twice to verify that it was not an artifact of incomplete reverse transcription.

Testis and sperm protein extract preparation, electrophoresis, and Western blot analysis

Freshly isolated testes were decapsulated and then Dounce homogenized on ice in RIPA buffer. Homogenates were kept at 4°C for 2 h with frequent vortexing, then centrifuged. After determination of supernatant protein concentrations and the addition of a cocktail of protease inhibitors, 100-μg aliquots were further prepared for gel electrophoresis. For sperm, freshly isolated cauda epididymides were minced, then incubated at 37°C in IVF medium (modified Krebs-Ringer-bicarbonate buffer containing 2% BSA, 1.7 mM Ca^{2+}, and 50 mM HEPES) (Olds-Clarke and Johnson, 1993) in 5% CO_2 in air for 20 min to allow sperm to swim out. After removal of epididymal tissue and debris by brief, low speed centrifugation, supernatants containing sperm were collected and sperm were counted. Supernatants were then centrifuged at 16,000 × *g*, sperm pellets were washed, then resuspended in RIPA buffer plus protease inhibitor cocktail at a concentration of 7.7×10^4 sperm/μl. Aliquots containing $\sim 1 \times 10^6$ sperm were further prepared for gel electrophoresis.

For electrophoresis, aliquots were resuspended in 1× SDS–PAGE sample buffer (Invitrogen) without reducing agent and boiled. After boiling and centrifugation, reducing agent (Invitrogen) was added to the supernatants and preformed 3–8%. Tris acetate polyacrylamide gradient gels (Invitrogen), mounted in an Xcell SureLock apparatus (Invitrogen), were immediately loaded. Gels were electrophoresed in 1× Tris acetate/SDS running buffer (Invitrogen) at 150 V constant for 60 min. Markers consisted of HiMark high molecular weight standards (Invitrogen), high molecular weight Rainbow standards (Amersham), and total *Chlamydomonas* flagellar proteins kindly provided by Drs. George B. Witman and Jovenal T. San Agustin, University of Massachusetts Medical School, Worcester, MA.

Proteins separated by electrophoresis were transferred to Immobilon-P PVDF membranes (Millipore) in 1× transfer buffer (Invitrogen) at 4°C, 30 V constant, for 1 h in the same apparatus reset for Western blotting. Membranes were then soaked briefly in methanol, dried thoroughly, wet in 20% methanol, then stained in Ponceau-S/5% acetic acid to detect total protein. Stained membranes were blocked in 5% modified dried milk (Genotech, St. Louis, MO) in TBS-T before being probed with an affinity-purified primary antiserum followed by a peroxidase-conjugated secondary antibody. After washing, the signal was visualized using an enhanced chemiluminescent system (Pierce, Rockford, IL) followed by exposure to CL-Xposure film (Pierce).

Fluorescent immunohistochemistry and immunocytochemistry

For immunohistochemistry, fresh cryosections of mouse testes 10 μm thick were briefly fixed in freshly made ice-cold 4% paraformaldehyde in 0.1 M cacodylate buffer, pH 7.3. After washing in cacodylate buffer and PBS three times, free aldehydes were blocked by immersion in 50 mM glycine/PBS for 5 min at room temperature to quench autofluorescence. Sections were then rinsed in three changes of PBS, permeabilized in 0.2% Triton X-100/1% goat serum/PBS, then incubated in blocking solution (5% BSA/10% goat serum/PBS) for 2 h at room temperature. The blocking solution was then removed, and 200–300 μl of a solution containing either primary antibody, preimmune serum, or nothing in 1% BSA/5% goat serum/PBS were added to each section. Sections were then incubated overnight at 4°C in a humid chamber followed by washing in three changes of 5% BSA/1% goat serum/PBS at 4°C for 10 min each change, and the addition of a 1:500 dilution of rhodamine-labeled goat-anti-rabbit secondary antibody (Jackson ImmunoResearch, West Grove, PA) in 5% BSA/PBS. Slides were incubated for 1 h at 4°C in a humid chamber, followed by 10 washes in ice-cold PBS for 10 min each wash. Sections were mounted in an anti-quenching mounting solution (Vectashield; Vector Laboratories, Burlingame, CA) containing DAPI for fluorescence microscopy with a Nikon Eclipse E800.

For immunocytochemistry, cauda epididymal sperm in IVF medium were centrifuged at 800 × *g*, and the sperm pellets were resuspended in 200 μl PBS. After counting, the sperm concentration was adjusted to 2×10^7/ml, and aliquots of 50 μl were pipetted into small PAP pen circles on polylysine-coated slides. These were then incubated in humid chambers for 10 min at room temperature. To extract mitochondria, half the slides were treated with a high pH solution (200 mM Tris–HCl pH 9.5/2 mM DTT/1% Triton X-100; Lindemann et al., 1992; Si and Okuno, 1999) in a humid chamber for 10 min at room temperature. Following the removal of excess liquid, high pH-treated and -untreated

sperm were fixed in freshly made 4% paraformaldehyde in PBS at 4°C for 1–2 h. Fixed, air-dried sperm were then immersed in chilled acetone for 10 min, re-dried, then washed in two changes of 0.1% Tween-20/PBS and one change of PBS. Antigens were then retrieved by boiling the slides in 10 mM citrate pH 6.0 for 10 min. After cooling, sections were washed several times in PBS followed by blocking in a solution of 5% BSA/10% goat serum/PBS for 4 h at room temperature. Following removal of the blocking solution, either primary antibody or preimmune serum diluted in blocking solution was added, and slides were incubated at 4°C overnight in humid chambers. The next day slides were washed three times in 0.1% Tween-20/PBS, after which a 1:500 dilution of Cy3-labeled goat-anti-rabbit secondary antibody (Jackson ImmunoResearch) in 1% BSA/5% goat serum/PBS was added to each slide. Slides were then incubated at room temperature for 3 h in the dark, followed by 10 washes in ice-cold PBS for 10 min each wash. Sections were then mounted in an anti-quenching mounting solution (Gel Mount; Biomeda, Foster City, CA) containing DAPI for fluorescence microscopy with a Nikon Eclipse E800.

Computational methods

Consensus secondary structures were determined with the program, PREDICT PROTEIN, an automatic service for protein database searches and the prediction of aspects of protein structure (Rost et al., 2003), and JPRED, a consensus method for protein secondary structure prediction (Cuff and Barton, 1999, 2000), both available through the EXPASY Web site (www.expasy.ch). Potentially significant conserved amino acid patterns were evaluated with the program PRATT, also at the EXPASY Web site.

Putative calmodulin binding sites in DNAHC8 orthologs were identified with the Calmodulin Database Binding Site Prediction and Analysis programs (Yap et al., 2000), located at the Cellular Calcium Information Server (http://www.calcium.uhnres.utoronto.ca). Based on the nature of experimentally verified target sites in the database, the program uses a variety of criteria (hydropathy, alpha-helical propensity, residue weight, residue charge, hydrophobic residue content, helical class, and occurrence of particular residues) to predict not yet experimentally identified targets.

Candidate phosphorylation sites in DNAHC8 were identified with the ELM program (Puntervoll et al., 2003) and were ranked for stability with the NetPhos 2.0 program (Blom et al., 1999), both also available at the EXPASY Web site. Criteria for identifying candidate residues whose phosphorylation was stable were similar to those used in Samant et al. (2002). Briefly residues that scored 0.8 or greater on a 0–1.0 scale (where the default for positive stable phosphorylation is 0.5) with NetPhos 2.0 were accepted as strong candidates.

Prediction and analysis of coiled coil structures was performed with the COILS2 program (Lupas, 1996), also available at the EXPASY Web site. Briefly, sequences were evaluated with a 21-residue scanning window and with both available matrices (MTK and MTIDK), using the option for equally weighting hydrophobic positions with hydrophilic residues. Results were graphically displayed.

To identify DHC homologs of DNAHC8 (both complete and partial), BLASTp was used (Altschul et al., 1990) with DNAHC8 (GenBank accession no. AF356520) as the query sequence. BLAST analyses were performed at the NCBI Web site (www.ncbi.nlm.nih.gov) Ninety-six highly homologous sequences (those with a zero *E*-value) were aligned with the multiple sequence alignment program, CLUSTAL W (http://bioweb.pasteur.fr/seqanal/interfaces/clustalw.html) (Thompson et al., 1994), which does not penalize terminal gaps.

Results

Only the isoform of DNAHC8 carrying the unique N-terminal extension and the full-length C-terminus accumulates to significant levels in both the testis and spermatozoa

We produced affinity-purified polyclonal antisera against several putatively antigenic peptide epitopes from various parts of the longest possible DNAHC8 coding region (AF356520) to determine which, if any, DNAHC8 isoforms were present in the testes and/or sperm of +/+ and *t/t* males (Fig. 2). Antiserum 1 (AS1) was raised against residues 64–78 (EGEAPHPEDPKLLSE) of DNAHC8 for the purpose of identifying all DNAHC8 isoforms containing the previously described unique N-terminus (N-terminal extension) (Samant et al., 2002). Western blots of testis and sperm protein extracts probed with AS1 exhibited a single polypeptide band >500 kDa, equally abundant in +/+ and *t/t* samples, and undetectable in protein extracts made from the testes of males homozygous for the previously described *Dnahc8*^{S} allele (hereafter referred to as the *Dnahc8*-null allele) which expresses very little, if any, *Dnahc8* mRNA (Fig. 2) (Fossella et al., 2000; Samant et al., 2002). Neither shorter exposures of the blot, nor loading less of each protein extract, nor running the gel for a longer period of time resulted in resolution of the original protein band into two or more bands of different but similar sizes (data not shown). These data suggested that only one DNAHC8 isoform contained the complete N-terminal extension, and it accumulated to equivalent steady state levels in the testes and sperm of both +/+ and *t/t* males. Contrary to our previous speculation that proteins carrying the N-terminal extension would be of low steady state abundance (Samant et al., 2002), this DNAHC8 isoform appeared to be plentiful.

In order to ascertain the nature of the C-terminus (full-length or truncated) belonging to the protein recognized by AS1, we probed Western blots equivalent to those hybridized

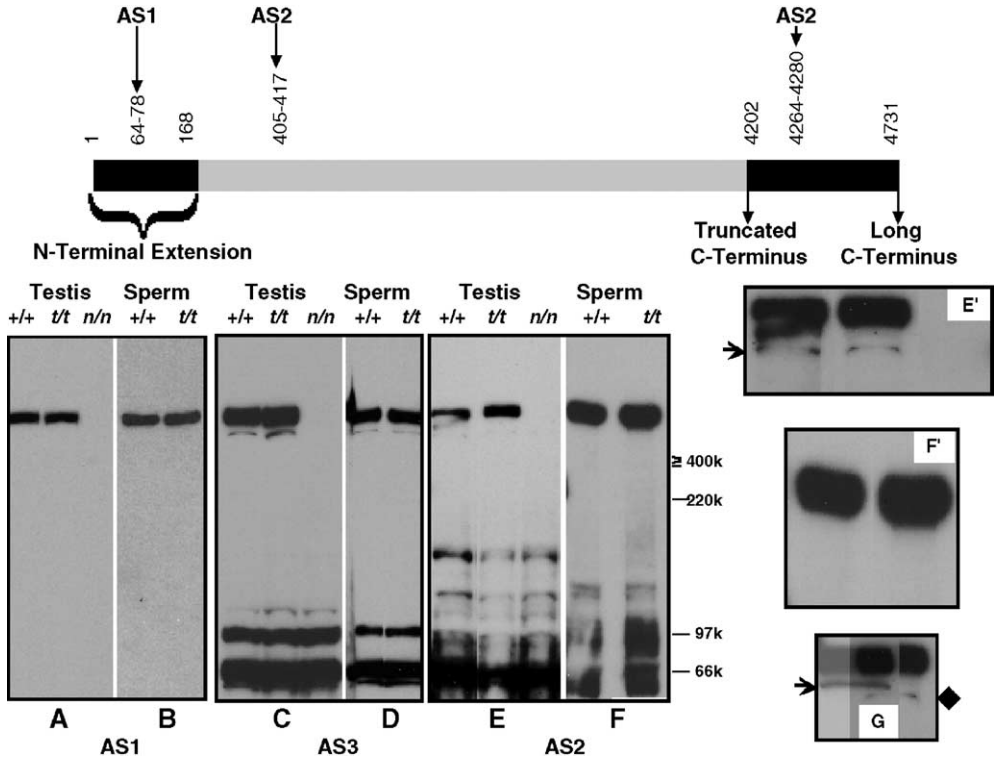

Fig. 2. Western blot analysis of DNAHC8 isoforms in testis and sperm from +/+ and *t/t* males. (Above) A linear diagram of the longest possible DNAHC8 isoform. Indicated are the amino acid positions and/or extent of the N-terminal extension, the truncated C-terminus, and the long C-terminus, as well as the positions of peptides against which antisera AS1, AS2, and AS3 were raised. (Below) Western blot analysis of testis (A, C, E), or sperm extracts (B, D, F) from males homozygous for wild-type (+/+), *t* haplotype (*t/t*), or null (*n/n*) alleles of *Dnahc8*. Probes were antisera AS1 (A, B), AS2 (E, F), or AS3 (C, D). Molecular weight markers are shown to the right of F. (Below right, from top to bottom) Long exposures of blots E (E′) and F (F′), and an overlap transparency of +/+ lane from C and *t/t* lane from E (G) indicating difference in size of short sperm DNAHC8 isoform (arrow) and testis-specific isoform (black diamond).

with AS1 with antiserum 3 (AS3), raised against residues 4264–4280 (RAGLKRTFAGINQDLLD) of DNAHC8^{+}, 62 amino acids downstream of the site of C-terminal truncation in putative "short" DNAHC8 isoforms (Fig. 2). AS3 recognized two polypeptide bands >500 kDa also of equal abundance in +/+ and *t/t* samples. The larger and considerably more plentiful of these appeared to be the same as the protein recognized by AS1. Because none of our three antisera was capable of immunoprecipitating DNAHC8, this could not be verified directly. However, both of the large polypeptides identified by AS3 appeared to be DNAHC8 isoforms, since they were not detectable in extracts made from the testes of males homozygous for the aforementioned *Dnahc8*-null allele. While this second polypeptide could be one without the N-terminal extension, it could also represent a weak cross-reaction with the γDHC paralog DNAHC5, recently found to localize specifically to the midpiece of the human sperm tail (Fliegauf et al., 2005). DNAHC5 could be degraded in *Dnahc8*-null testis and sperm, since the sperm tail in these mutants is not assembled (Pilder et al., 1993; Fossella et al., 2000; Samant et al., 2002). Alternatively, since DHCs are notoriously sensitive to proteolysis, this isoform could just as likely be an N-terminal proteolytic biproduct of the larger, considerably more abundant isoform.

Several abundant proteins banding below ~150 kDa (less abundant in sperm than testis) were also detected by AS3. Since these polypeptides were equally abundant in extracts made from the testes of males homozygous for the *Dnahc8*-null allele, it appeared that AS3 recognized products whose origins, though unknown, were not *Dnahc8* specific.

Antiserum 2 (AS2), raised against residues 405–417 (QMRKEADDSGPLT), was designed to identify all DNAHC8 isoforms predicted by our earlier *Dnahc8* mRNA results (Samant et al., 2002). At first glance, AS2 appeared to give almost identical results to AS1 for proteins in the ~500 kDa range (Fig. 2): a single polypeptide banding at >500 kDa (not detected in *Dnahc8*-null extracts and equally abundant in +/+ and *t/t* samples), the same size and relative abundance as the protein recognized by AS1. However, a closer inspection of the blot indicated the presence of a very weak band in testis extracts from +/+ and *t/t* animals, apparently absent not only from *Dnahc8*-null testis extracts, but from +/+ and *t/t* sperm extracts. Longer blot exposures (~1 h) confirmed the presence of this polypeptide band in testis extracts only (Figs. 2E′ and F′). This putative DNAHC8 variant also appeared to be slightly smaller than the shorter, non-abundant testis/sperm isoform identified by

AS3 (Fig. 2). Because the shorter testis/sperm isoform identified by AS3 was not also identified by AS2, it would have to contain an N-terminal ultimate residue C-terminal to amino acid 417. As was the case for AS3, several proteins smaller than ~150 kDa, present also in *Dnahc8*-null extracts, were identified by AS2.

Overnight exposures of blots probed with AS2 produced a barely detectable band in the *Dnahc8*-null testis extract lane of approximately the same size as the testis-restricted band from DNAHC8-expressing extracts (data not shown). Because our *Dnahc8*-null animals are not deleted for *Dnahc8* (Samant et al., 1999), but instead carry a highly polymorphic, grossly underexpressed *Dnahc8* allele from *Mus spretus*, leaky expression of one or more isoforms of DNAHC8 is possible. Alternatively, AS2 might weakly recognize an epitope of another DHC band of approximately equal size, such as the cytoplasmic DHC1, also present in testis and not sperm.

The accumulated data argue that the abundant isoform of DNAHC8, recognized by all three antisera, is an authentic in vivo polypeptide, but that the smaller, extremely minor isoforms are either proteolytic artifacts of this larger isoform, or antisera cross-reactions with other DHCs or their proteolytic biproducts. If the testis-restricted isoform is not a proteolytic artifact, it might represent the DNAHC8 variant with the truncated C-terminus, since it is, as was predicted for that putative isoform, non-abundant (Samant et al., 2002). The existence of nearly identical variant mRNA isoforms coding for C-terminally truncated DNAHC8 molecules from both mouse and human testes (GenBank Accession Nos. AF356521, AF356523, AF363577, AF527623) lend support to the idea that such DNAHC8 isoforms are

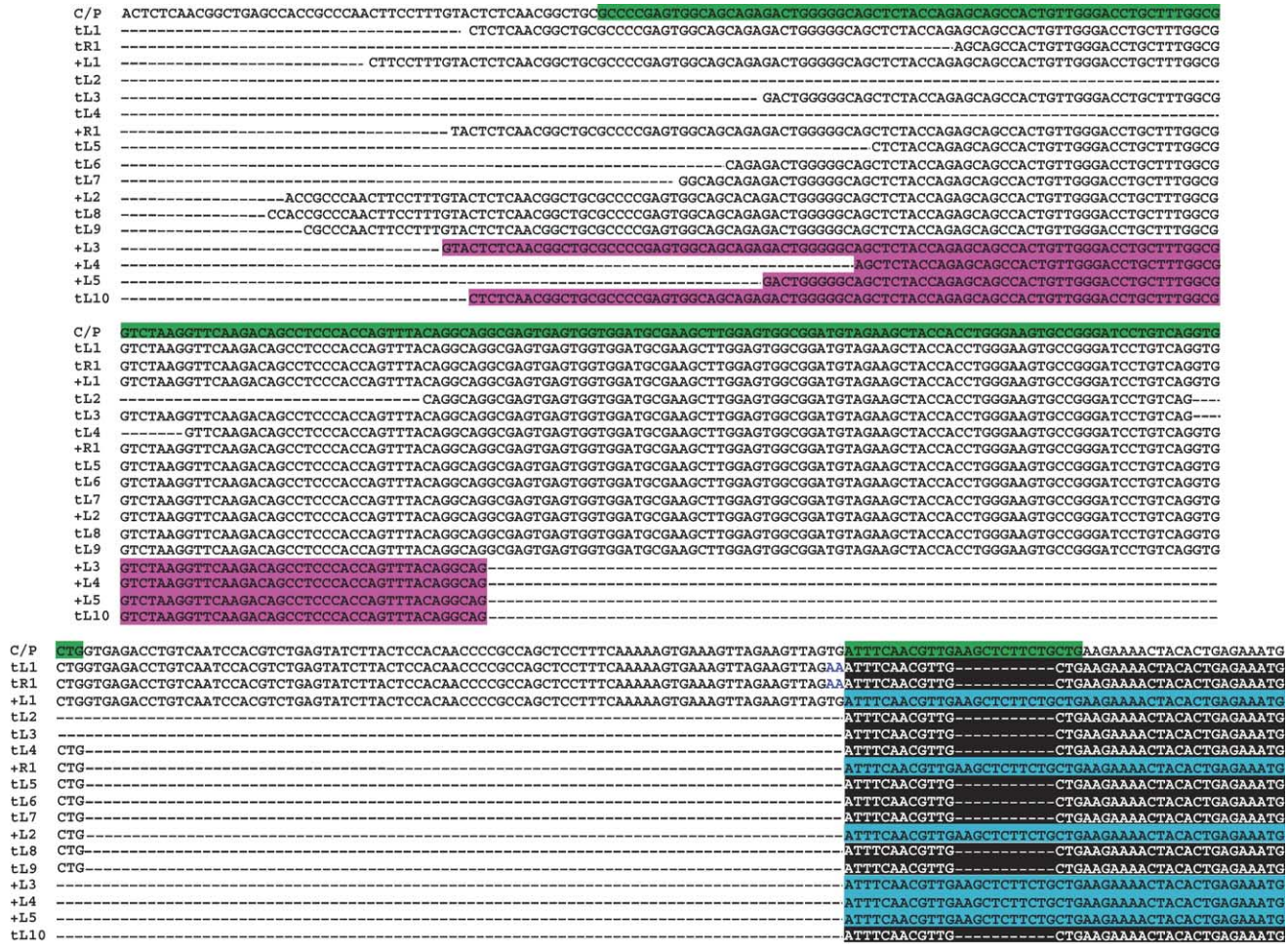

Fig. 3. Alignment of 5′UTRs of *Dnahc8*$^{+}$ and *Dnahc8*^{t} mRNAs. Top sequence (C/P) represents a consensus 5′-end including some promoter region sequence with first exon probe sequence from Samant et al. (2002) highlighted in green. Sequences are named for whether they were isolated from wild-type (+) or *t* haplotype (*t*) mRNA and from cDNA libraries (*L*) or by RT-PCR (*R*). All 5′-ends were isolated at least twice with those highlighted in purple being isolated most frequently, and all others about equally. *+R1*, *tR1*, and *tL1* are from Samant et al. (2002). *tL2** is not the same as *tL2* seen in Samant et al. (2002), which was the only 5′-end ever isolated initiating downstream of the first in-frame methionine in exon 2. All first exons isolated in this experiment splice to the same second exon represented by the black (*t*) and turquoise (+) highlighted sequences.

produced in the testis and are specific to late meiotic/early spermiogenic cells. However, because the testis-restricted isoform recognized by AS3 is not visualized with AS1 as well, it could not contain the full-length N-terminal extension previously predicted for C-terminally truncated isoforms by in situ hybridization and northern analyses (Samant et al., 2002). Thus, its identity as the C-terminally truncated isoform remains questionable. Finally, because no difference is apparent between proteins from +/+ or *t/t* animals vis-a-vis the size and abundance of any of the identified DNAHC8 isoforms, we conclude that putative DNAHC8^{t} defectiveness is unlikely to be a biproduct of a lack of abundance or instability.

The existence of numerous Dnahc8 mRNAs coding for the complete N-terminal extension with different 5′UTRs

Previous results had suggested that mouse *Dnahc8* mRNAs coding for isoforms with the complete N-terminal extension were of low steady-state abundance (Samant et al., 2002). Thus, we were surprised by the result showing that the only DNAHC8 isoform containing the N-terminal extension was not only a full-length isoform, but the only one that was abundant. A likely explanation for the apparent profusion of this DNAHC8 variant was suggested by our isolation of human *Dnahc8* (*DNAH8*) orthologous cDNAs showing that at least two *DNAH8* mRNAs existed with completely different 5′UTRs, both of them coding for proteins carrying the human version of the N-terminal extension (GenBank accession nos. AF527621, AF527622). This result suggested that the mouse DNA construct (made from a *Dnahc8*$^{+}$ 5′UTR) with which messages coding for the N-terminal extension had been probed (Samant et al., 2002) may have hybridized to only a subset of such mRNA isoforms.

Extensive cloning of *Dnahc8* 5′-ends from mouse +/+ and *t/t* testis cDNA libraries prepared by both oligo-dT and random priming revealed that numerous short +/+ and *t/t* 5′UTRs (“first” exons) existed (Fig. 3), all splice variants of the previously described, larger 5′UTR used for probing Northern blots (Samant et al., 2002). The shortest varieties appeared, by virtue of their repeated isolation, to be more abundant than the longer 5′-ends, and all newly isolated “first” exons spliced to the same second exon from which translation of the N-terminal extension was initiated. Because many of the more abundant forms were very short in relationship to the original probe sequence (Samant et al., 2002), high stringency washing of Northern blots in that previous study may have produced a result suggesting that mRNAs coding for the N-terminal extension were of low abundance, when probably all or nearly all *Dnahc8* mRNAs encode it. This result also explained why previous northern analyses of mouse *Dnahc8* mRNAs never produced more than a single-size band in both wild-type and *t* (Samant et al., 2002).

Light microscopic fluorescent immunolocalization of the DNAHC8 isoform with the N-terminal extension is identical in the testes of +/+ and t/t animals

Because Western blotting confirmed that AS1 specifically recognized a single DNAHC8 polypeptide, we were able to use it to immunolocalize the most abundant form of DNAHC8 in testis sections from +/+ and *t/t* mice. In both, intense fluorescent signal was seen in sperm tails within the seminiferous tubule lumens, where the more distal region of the tails normally accumulate (Fig. 4). In addition, individual fluorescent sperm tails could be seen in the fainter cytoplasm surrounding the tubule lumens, but fluorescence associated with tails diminished dramatically more proximal to the elongating sperm heads. These observations suggested that isoforms of DNAHC8 with the complete N-terminal extension localize specifically to the distal region (possibly the principal piece) of the sperm tail. In addition, in both +/+ and *t/t* mice, bright punctate fluorescence appeared in the cytoplasms of many primary spermatocytes (Fig. 4, lower insets). Moreover, in some round spermatids, localized intense signal was seen in structures suggestive of newly forming flagella (Fig. 4, upper insets). In similar sections exposed to preimmune

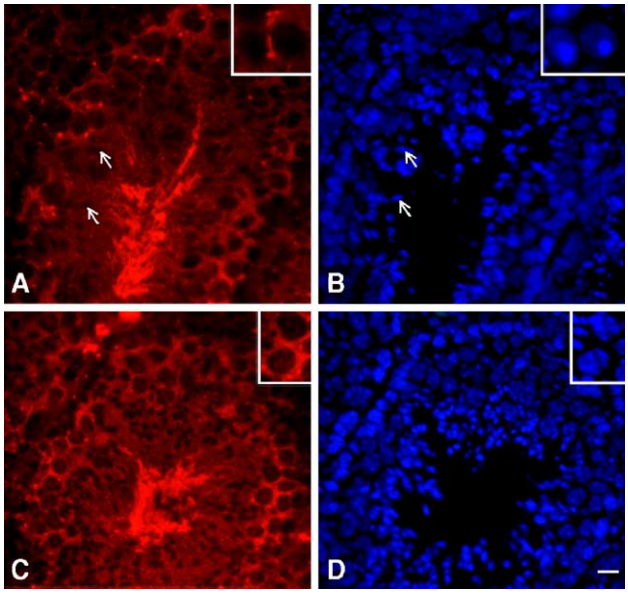

Fig. 4. Testis sections from +/+ (A, B) and *t/t* (C, D) mice subjected to immunofluorescent localization for the DNAHC8 isoform with the N-terminal extension with AS1 (A, C) or exposed to DAPI to visualize nuclear morphology (B, D). Both views show areas in spermatogenic stages IX–X. Brightest fluorescence occurred in both animal models in distal tails within tubule lumens, with a diminished fluorescence over tails nearer to the sperm nuclei (arrows in A and B indicate nuclei), suggesting a specific localization to the principal piece of the sperm tail. In addition, fluorescence was seen in punctuate areas within primary spermatocytes (insets C, D). In tubules in earlier stages of spermatogenesis where round spermatids were present, bright fluorescence also occurred over structures which appear to be portions of newly forming tails (insets A, B). Essentially no seminiferous tubule-associated fluorescence was seen in sections exposed to preimmune serum rather than primary antibody (not shown). Scale bar = 10 μm.

serum rather than to primary antibody, little fluorescence was seen over any portions of seminiferous tubules (data not shown).

The DNAHC8 isoform with the N-terminal extension is confined to the principal piece of the cauda epididymal sperm flagellum

To test the hypothesis that DNAHC8 isoforms with the N-terminal extension are specifically associated with the principal piece of the sperm tail, sperm of both genotypes were collected from isolated cauda epididymides, then fixed, permeated, and subjected to immunofluorescence as for testis sections. Sperm of both genotypes exhibited bright, intense fluorescence over the principal piece of the tail with little if any fluorescence over the midpiece (Figs. 5A–D). To rule out the possibility that the mitochondrial sheath limited antibody penetration into the axoneme in the midpiece, we also extracted mitochondrial sheaths from midpieces prior to sperm fixation (Lindemann et al., 1992; Si and Okuno, 1999). Resulting sperm lacking their mitochondrial sheaths were readily identifiable by an obvious visible reduction in the circumference of their midpieces. Even after removal of the mitochondrial sheaths from these sperm, no fluorescence was seen over the midpiece following immunolocalization for DNAHC8 (Figs. 5E–H). However, immunolocalization of β-tubulin produced fluorescence over the entire sperm tail, even in sperm lacking the mitochondrial sheath (Figs. 5K and L). These findings, taken together with our observations of DNAHC8 localization in testicular sperm, indicate that there is no difference in subcellular location of the protein between *t/t* and +/+ mice. Furthermore, they suggest that the DNAHC8 isoform with the complete N-terminal extension is limited to a specific compartment of the flagellum in mature sperm of both +/+ and *t/t* animal. Since the subunit composition of the ODA in well-studied protozoan flagella and cilia appears to be invariant along the length of the flagellum, our present findings, along with recent studies showing that the γDHC paralog, DNAHC5, is located exclusively in the midpiece of the human sperm axoneme, indicate a new level of ODA structure–function complexity in the mammalian sperm tail.

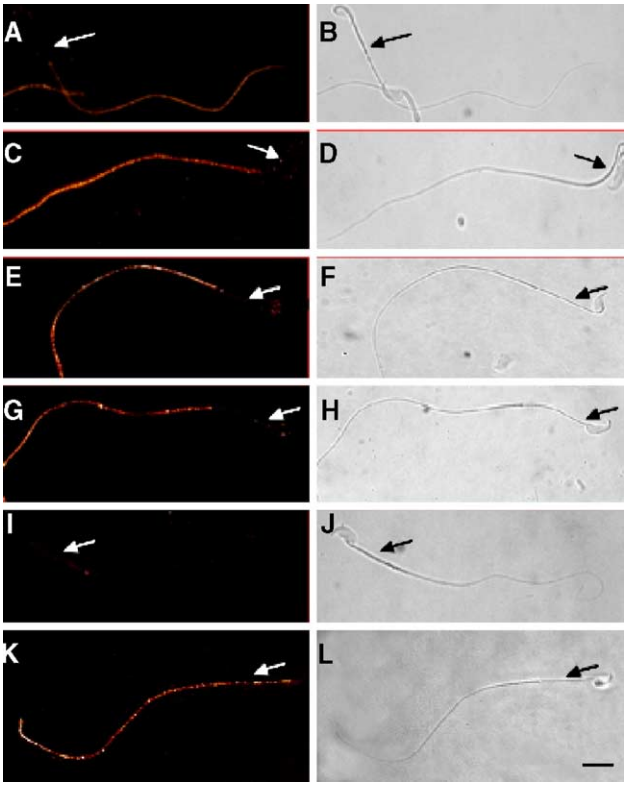

Fig. 5. Phase contrast images (right) and immunofluorescent localization (left) of the DNAHC8 isoform with the N-terminal extension in isolated cauda epididymal sperm from +/+ (A, B, E, F) and *t/t* mice (C, D, G, H) without (A–D) or with (E–H) prior extraction of mitochondria. Arrows indicate location of the midpieces in representative sperm. In both untreated and extracted sperm, the long isoform of DNAHC8 localizes exclusively to the principal piece, with little fluorescence over the midpiece. (I, J) Sperm exposed to preimmune serum in place of primary antibody. (K, L) Extracted sperm probed with anti-tubulin antibody. Scale bar = 10 μm.

Comparative computational analyses of DNAHC8^t aligned with wild-type DHCs suggest that three of the seventeen DNAHC8^t mutations are primary candidates for DNAHC8 dysfunction

To determine potential significance of any of the seventeen missense mutations in DNAHC8^t, we have examined each with respect to (1) the conservation of its wild-type counterpart in 96 full-length DHC sequences, (2) the normal frequency of substituting it for its wild-type counterpart (Topham et al., 1993), and (3) its potential effects on local structural properties that might impinge on normal DNAHC8 function. These *in silico* examinations have resulted in the selection of three mutations, one in the N-terminal extension and two in the motor unit that will serve as primary candidate mutations for future investigation. However, at present we cannot rule out the possibility that DNAHC8^t dysfunction results in good measure from the mass action of many of the more subtle mutations in the stem, some of which appear in clusters.

The first candidate mutation, a glycine (G) to arginine (R) change at residue 127 ($G_{127}R$) in mouse, resides within the N-terminal part of an almost completely conserved amino acid pattern (average identity = 81%, average conservation = 97.5%) of unknown function, this pattern comprising the C-terminal ~25% of the N-terminal extension of all mammalian orthologs (Fig. 6). Pattern dissection indicates conservation of numerous serines in its N-terminal half followed closely by a 14-3-3 adaptor-binding ligand whose C-terminus overlaps the N-terminus of an IQ calmodulin target motif. Both motifs are known to interact with other proteins via shifts in local secondary structure, often caused by vicinal residue phosphorylation (Rosenquist et al., 2000; Wu et al., 2003; Krajewski et al., 2003; Browne

Fig. 6. Alignment of a highly conserved mammalian pattern in the C-terminal ~25% of the N-terminal extensions of DNAHC8 orthologs (see below alignment) including, from top to bottom: *M. musculus* wild-type, *M. musculus t* haplotype, *R. norvegicus*, *H. sapiens*, *P. troglodytes*, *C. familiaris*, *B. taurus*, and the non-mammalian *G. gallus* ortholog. Amino acid identities are represented by yellow letters on a black background, conservative changes by white letters on a blue background, and non-conservative differences by black letters on a yellow background. Standard for comparison is *M. musculus* wild-type. Vertical red and orange lines represent truncations of the conserved pattern at its N-terminus when either the mDNAHC8^t sequence or the *G. gallus* sequence is analyzed together with the wild-type mammalian sequences. Boxed sequence represents the potential IQ motif conserved in all orthologs so far identified. Lowercase sequences with dashed line above represent 14-3-3 binding ligand motifs conserved in mammalian orthologs, while solid line above sequences represents a conserved PKA phosphorylation site. Italicized conserved serines indicated by purple diamonds above alignment represent amino acids in overlapping kinase motifs which may be stably phosphorylated. Conserved non-italicized serines indicated by orange and yellow diamonds above alignment represent amino acids whose phosphorylation is predicted to be substantially stabilized in mDNAHC8^t due to the G→R mutation whose position is indicated by the filled box above the alignment.

and Proud, 2004; Xang, 2005). The high level of conservation of this region among wild-type DNAHC8 orthologs, its lack of homology to the N-termini of all other DHCs, and the possibility that the *t* mutation may substantially affect changes in local peptide conformation and putative protein–protein interactions via its ability to stabilize potential vicinal phosphorylation events (Betts and Russell, 2003) suggest its possible importance to DNAHC8-specific stem unit functions/interactions in mammals.

The first two motor mutations (V to alanine (A) at residue 2224 [$V_{2224}A$] and proline (P) to threonine (T) at residue 3408 [$P_{3408}T$]) occur in regions highly conserved with annotated functional significance in wild-type DHCs, thus constituting the second and third primary candidates for DNAHC8^t dysfunction. The first is located in Helix 6 (H6) of Box VII′ in the AAA1 C-domain, part of the most highly conserved AAA module of the dynein motor unit (the site of both ATP binding and hydrolysis). Our alignment of wild-type DHCs demonstrates that V is highly conserved at this position. V and isoleucine (I), its most frequent substitute in other proteins, are represented in 89/96 chains examined (see Supplemental Figs. 1 and 2). All seven of the other wild-type DHCs contain residues with bulky side chains. Alanine represents 0/96 aligned residues, suggesting its unsuitability as a substitute amino acid at the position in question, despite ranking as the second most frequent alternate for V (Topham et al., 1993). Since the V/I conservation level of nearly 93% is well above the 66% average conservation level for residues in AAA modules (Mocz and Gibbons, 2001), and A is not found at this position, we propose that A is most likely detrimental to proper motor function in γDHCs as well as most other DHC subtypes.

The second DNAHC8^t motor mutation ($P_{3408}T$) occurs at the end of the outward α-helical branch of the anti-parallel coiled-coil stalk upon which the ATP-dependent microtubule binding site (MBS) sits (Samant et al., 2002), and aligns with a residue formerly reported to play an important role in ATP-sensitive microtubule binding in cytoplasmic DHCs (Koonce and Tikhonenko, 2000). In our alignment of wild-type DHCs, the altered residue is T in only ~1% of wild-type DHCs, but P in ~25%, including all wild-type metazoan γDHCs. The conservation of proline at this site reflects a potentially significant effect of the mutation on DNAHC8$^+$/MBS structure/function. Because of the known P effects on α-helical structure, we analyzed the proclivity of P to terminate the outward α-helical branch of the MBS stalk coiled-coil in wild-type DHCs relative to the DNAHC8^t T with the Coils program (Lupas, 1996). The result strongly suggested that outward helical termination occurs at least two residues earlier in γ and other DHCs with P at this position than in DNAHC8^t with T (data not shown), suggesting that T in the DNAHC8^t outward helix might cause a three-dimensional alteration of the MBS or a misalignment of return and outward stalk α-helices.

Discussion

A stable DNAHC8 isoform is expressed in primary spermatocytes and targeted to the principal piece of the sperm tail in +/+ and t/t males

Three putative DNAHC8 isoforms have been identified in this study (Fig. 2), two specific for both testis and sperm and one restricted to the testis. Both of the testis/sperm isoforms appear to carry the DNAHC8 full-length C-terminus (Samant et al., 2002), but vary from each other by their relative abundance and the composition of their N-termini. The less abundant of the two may be a proteolytic artifact of its more bountiful counterpart, an antiserum cross-reaction with another DHC, or an authentic in vivo isoform of DNAHC8. Due to the known sensitivity of DHCs to proteolysis and the existence of limited regions of high homology between related DHC sequences, neither of the first two possibilities can be ruled out. In addition, the testis-restricted, barely visible isoform identified on Western blots with AS2 might be the formerly proposed C-terminally truncated DNAHC8 polypeptide (Samant et al., 2002);

however, its appearance could represent a very weak cross reaction of AS2 with the cytoplasmic DHC1, present also in testis but not sperm.

Neither of the two barely visible isoforms contain the complete N-terminal extension as does the abundant isoform recognized on Western blots by all three of our antisera. Our determination that all *Dnahc8* 5′UTR exons so far isolated from both +/+ and *t/t* testis cDNA libraries splice to the exon from which translation of the N-terminal extension is initiated (Fig. 3) strongly support the idea that these scarcely detectable putative DNAHC8 isoforms are little more than proteolytic derivatives of the abundant full-length isoform. Thus, in the absence of substantive experimental evidence showing that one or both are genuine products of post-translational processing, the in vivo authenticity of the two smaller isoforms detected by Western blot must be viewed with skepticism at this time.

Our immunohistochemical studies indicate that the abundant DNAHC8 isoform (hereafter referred to simply as DNAHC8) first appears in the cytoplasm of primary spermatocytes (Fig. 4), in support of previously published findings implying that *Dnahc8* translation must occur in those cells (Samant et al., 2002). As suspected, DNAHC8 is also visible in some round spermatids along the cell periphery, possibly at the site of the budding tail (Fig. 4), and in elongating spermatids. There, DNAHC8 appears primarily in the distal portion of the developing tail toward the center of the lumen of the seminiferous epithelium (Fig. 4), suggesting that its location is the principal piece of the sperm tail. Restriction of DNAHC8 to this subcellular destination was confirmed by additional immunocytochemical studies of epididymal sperm from both +/+ and *t/t* males (Fig. 5). These data make it clear that none of the seventeen missense mutations identified in DNAHC8^t have a demonstrable effect on its expression, abundance, or subcellular localization. This is not surprising since the same large deletion of part of the DNAHC5 motor unit that causes its mislocalization in human respiratory cilia, causes sperm immotility, but not mislocalization in sperm tails (Fliegauf et al., 2005).

Because DNAHC8 is a member of the γDHC subfamily, and thus a putative subunit of the ODA, its subcellular localization exclusively to the principal piece of the sperm tail was at first surprising. This reaction was due to the unanticipated variability of ODA DHC composition in the mammalian sperm axoneme, in contrast to its invariable nature in more primitive flagellated cell types like *Chlamydomonas reinhardtii*. We derived two simple alternative explanations for this unexpected phenomenon: either (1) the ODA of mammalian sperm tails were compartmentally variable in their DHC composition to provide independent regulation of movement in the midpiece and principal piece when necessary; or (2) duplication of ODA DHC genes in mammals and birds had resulted in the development of novel IDA DHC subtypes in sperm tails modeled on ODA DHC prototypes. A recent report suggests that the truth is closer to the first explanation, but is somewhat more complex. Fliegauf et al. (2005) demonstrated that the ODA of the human sperm flagellum and respiratory cilium both show proximal vs. distal compartment specificity in their DHC composition, and that the combination of ODA DHCs in the different compartments of each is cell type specific. Thus, the ODA of the mammalian sperm tail possess a single βDHC along the length of the axoneme, but two γDHCs, one in the midpiece (DNAHC5) and the other in the principal piece (identified in the present study as DNAHC8). In a similar fashion, the ODA of mammalian respiratory cilia have a single γDHC (DNAHC5), but two βDHCs, one proximal and one distal. Built into this doubly novel paradigm of cell type-specific mechanisms capable of independently regulating the proximal and distal portions of the flagellum/cilium is preservation of the basic ultrastructural architecture of the axonemal engine.

DNAHC8 is one of several principal piece-specific flagellar components of mammalian sperm. Others include CATSPER1, an ion channel specific to the plasma membrane surrounding the principal piece (Ren et al., 2001), and a large cohort of glycolytic and signaling molecules (Blake et al., 1995; Vijayaraghavan et al., 1999; Mei et al., 1997; Mori et al., 1998; Bunch et al., 1998; Carr et al., 2001), either part of or anchored to the periaxonemal fibrous sheath (FS). Because DNAHC8 is a motor component of the axonemal circumference itself, it is likely to act as a final filter through which principal piece-specific periaxonemal signals regulating flagellar activity are interpreted. As such, DNAHC8^t could represent an errant cipher of coded information controlling the flagellar beat of the principal piece, leading to its chronic negative curvature as is observed in sperm from *t/t* but not +/*t* males (Olds-Clarke and Johnson, 1993). This also implies that the putative detrimental effect of DNAHC8^t is fully complemented in +/*t* males, signifying that its expression is probably not related to the TRD phenotype. Interestingly, the principal piece specificity of DNAHC8 also reinforces the hypothesis that DNAHC8^t is only partially responsible for the expression of "curlicue" (Redkar et al., 1998), a phenotype involving aberrant curvature of both the midpiece and principal piece of the mouse sperm tail (Olds-Clarke and Johnson, 1993).

Potential effects of mutations in DNAHC8^t

Three characteristics of DNAHC8 separate it from DNAHC5. These include its cell type (testis/sperm) specificity, its principal piece exclusivity, and its highly unique extended N-terminus (Samant et al., 2002). Theoretically, this flexible N-terminal "appendage" would allow DNAHC8 to interact differently from DNAHC5 with the single β DHC and the ODA repertoire of DLCs (dynein light chains) and DICs (dynein intermediate chains) in the sperm flagellum. The testis/sperm specificity, compartmental location, and axonemal circumferential position of DNAHC8 also suggest that this novel N-terminus is capable

of associating, either directly or through intermediaries, with glycolytic enzymes and signal transduction molecules that are anchored to or interact with elements of the peria-xonemal fibrous sheath (FS) (Samant et al., 2002).

The C-terminal 25% of the N-terminal extension (Fig. 6) contains a highly conserved amino acid pattern in mammalian DNAHC8 orthologs carrying several consensus phosphorylation and overlapping protein binding motifs, as well as the first DNAHC8^t mutation, a G to R change at residue 127. Because at least one (and possibly both) of these protein binding sequences (a potential 14-3-3 affinity ligand and a putative IQ calmodulin target region) is known to regulate interactions with binding partners via vicinal residue phosphorylation (Rosenquist et al., 2000; Wu et al., 2003; Krajewski et al., 2003; Browne and Proud, 2004; Xang, 2005), it is tempting to speculate that similar events within this highly conserved region might modulate the competition between proteins for binding to these overlapping sites (Yoo et al., 2004). Thus, a mutation that alters the normal phosphorylation pattern of this region, such as is predicted for the $G_{127}R$ mutation in DNAHC8^t, could have profound consequences on DNAHC8 activity.

The last two DNAHC8^t dysfunction candidate mutations we have considered are universal to all DNAHC8^t isoforms, including those that may be proteolytic artifacts. The first of these is the first motor unit mutation, occurring in H6 of Box VII′ of the highly conserved AAA1 C-domain ($V_{2224}A$). Models of AAA structure have described H6 as part of the AAA C-terminal domain that forms the hydrophobic nucleotide binding cleft, linking nucleotide binding and/or hydrolysis to the production and propagation of conformational changes within the dynein motor unit (Neuwald et al., 1999; Mocz and Gibbons, 2001). Regardless of the fact that A is considered a stronger helix-favoring residue than either V or I (Williams et al., 1987), we propose that in H6 of AAA1, a residue with a branched β-carbon (or in 4/96 cases, another bulky side chain) at the position in question, and a completely conserved I approximately one turn of H6 more proximal, are required to facilitate motor unit activity, possibly because they are better able than A to affect productive packing interactions with other residues during nucleotide-induced conformational changes.

The last candidate mutation is located in the motor unit at the very N-terminus of the MBS ($P_{3408}T$). Our analysis suggests that this alteration is harmful to the function of DNAHC8, due to its ability to promote an impaired conformation of the MBS. This hypothesis is reinforced by a previous study showing that alteration of the residue at this position in cytoplasmic DHCs has a deleterious effect on ATP-sensitive MT binding (Koonce and Tikhonenko, 2000).

Acknowledgments

SHP would like to thank Dr. Charles Lindemann, Oakland University, for many enlightening conversations about the biophysics of flagellar motility, and Drs. George Witman and Jovenal T. San Agustin for the kind gift of *Chlamydomonas reinhardtii* flagellar protein extracts. This work was supported by a grant to SHP from the National Institutes of Health (R01-HD31164).

Appendix A. Supplementary data

Supplementary data associated with this article can be found, in the online version, at doi:10.1016/j.ydbio.2005.06.002.

References

Altschul, S.F., Gish, W., Miller, W., Myers, E.W., Lipman, D.J., 1990. Basic local alignment search tool. J. Mol. Biol. 215, 403–410.

Bartolome, C., Maside, X., 2004. The lack of recombination drives the fixation of transposable elements on the fourth chromosome of *Drosophila melanogaster*. Genet. Res. 83, 93–100.

Betts, M.J., Russell, R.B., 2003. Amino acid properties and consequences of substitutions. In: Barnes, M.R., Gray, I.C. (Eds.), Bioinformatics for Geneticists. John Wiley and Sons, New York, pp. 289–316.

Blake, J.A., Eppig, J.T., Richardson, J.E., Davidson, M.T., 1995. The mouse genome database: expanding genetic and genomic resources for the laboratory mouse. Nucleic Acids Res. 28, 108–111.

Blom, N., Gammeltoft, S., Brunak, S., 1999. Sequence and structure-based prediction of eukaryotic protein phosphorylation sites. J. Mol. Biol. 294, 1351–1362.

Browne, G.J., Proud, C.G., 2004. A novel mTOR-regulated phosphorylation site in elongation factor 2 kinase modulates the activity of the kinase and its binding to calmodulin. Mol. Cell. Biol. 24, 2986–2997.

Bunch, D.O., Welch, J.E., Magyar, P.L., Eddy, E.M., O'Brien, D.A., 1998. Glyceraldehyde 3-phosphate dehydrogenase-S protein distribution during mouse spermatogenesis. Biol. Reprod. 58, 834–841.

Carlson, A.E., Westenbroek, R.E., Quill, T., Ren, D., Clapham, D.E., Hille, B., Garbers, D.L., Babcock, D.F., 2003. CatSper1 required for evoked Ca2+ entry and control of flagellar function in sperm. Proc. Natl. Acad. Sci. U. S. A. 100, 14864–14868.

Carr, D.W., Fujita, A., Stentz, C.L., Liberty, G.A., Olson, G.E., Narumiya, S., 2001. Identification of sperm-specific proteins that interact with A-kinase anchoring proteins in a manner similar to the type II regulatory subunit of PKA. J. Biol. Chem. 276, 17332–17338.

Chapelin, C., Duriez, B., Magnino, F., Goossens, M., Escudier, E., Amselem, S., 1997. Isolation of several human axonemal dynein heavy chain genes: genomic structure of the catalytic site, phylogenetic analysis and chromosomal assignment. FEBS Lett. 412, 325–330.

Cuff, J.A., Barton, G.J., 1999. Evaluation and improvement of multiple sequence methods for protein secondary structure prediction. Proteins 34, 508–519.

Cuff, J.A., Barton, G.J., 2000. Application of multiple sequence alignment profiles to improve protein secondary structure prediction. Proteins 40, 502–511.

Fliegauf, M., Olbrich, H., Horvath, J., Wildhaber, J.H., Zariwala, M.A., Kennedy, M., Knowles, M.R., Omran, H., 2005. Mis-localization of DNAH5 and DNAH9 in respiratory cells from primary ciliary dyskinesia patients. Am. J. Respir. Crit. Care Med., 1343–1349 (electronic publication ahead of print).

Fossella, J., Samant, S.A., Silver, L.M., King, S.M., Vaughan, K.T., Olds-Clarke, P., Johnson, K.A., Mikami, A., Vallee, R.B., Pilder, S.H., 2000. An axonemal dynein at the *Hybrid Sterility 6* locus: implications for t haplotype-specific male sterility and the evolution of species barriers. Mamm. Genome 11, 8–15.

Hammer, M.F., Schimenti, J., Silver, L.M., 1989. Evolution of mouse chromosome 17 and the origin of inversions associated with *t* haplotypes. Proc. Natl. Acad. Sci. U. S. A. 86, 3261–3265.

Ho, H.C., Suarez, S.S., 2003. Characterization of the intracellular calcium store at the base of the sperm flagellum that regulates hyperactivated motility. Biol. Reprod. 68, 1590–1596.

Koonce, M.P., Tikhonenko, I., 2000. Functional elements within the dynein microtubule-binding domain. Mol. Biol. Cell 11, 523–529.

Krajewski, J.L., Luetje, C.W., Kramer, R.H., 2003. Tyrosine phosphorylation of rod cyclic nucleotide-gated channels switches off Ca2+/calmodulin inhibition. J. Neurosci. 23, 10100–10106.

Lindemann, C.B., Orlando, A., Kanous, K.S., 1992. The flagellar beat of rat sperm is organized by the interaction of two functionally distinct populations of dynein bridges with a stable central axonemal partition. J. Cell Sci. 102, 249–260.

Lindemann, C.B., Kanous, K.S., 1997. A model for flagellar motility. Int. Rev. Cytol. 173, 1–72.

Lupas, A., 1996. Predicting coiled-coil regions in proteins. Curr. Opin. Struct. Biol. 7, 388–393.

Lyon, M.F., 1984. Transmission ratio distortion in mouse t-haplotypes is due to multiple distorter genes acting on a responder locus. Cell 37, 621–628.

Lyon, M.F., 1986. Male sterility of the mouse t-complex is due to homozygosity of the distorter genes. Cell 44, 357–363.

Lyon, M.F., 2003. Transmission ratio distortion in mice. Annu. Rev. Genet. 37, 393–408.

Marquez, B., Suarez, S.S., 2004. Different signaling pathways in bovine sperm regulate capacitation and hyperactivation. Biol. Reprod. 70, 1626–1633.

Mei, X., Singh, I.S., Erlichman, J., Orr, G.A., 1997. Cloning and characterization of a testis-specific, developmentally regulated A-kinase-anchoring protein (TAKAP-80) present on the fibrous sheath of rat sperm. Eur. J. Biochem. 246, 425–432.

Mocz, G., Gibbons, I.R., 2001. Model for the motor component of dynein heavy chain based on homology to the AAA family of oligomeric ATPases. Structure (Camb.) 9, 93–103.

Mori, C., Nakamura, N., Welch, J.E., Gotoh, H., Goulding, E.H., Fujioka, M., Eddy, E.M., 1998. Mouse spermatogenic cell-specific type 1 hexokinase (mHk1-s) transcripts are expressed by alternative splicing from the mHk1 gene and the HK1-S protein is localized mainly in the sperm tail. Mol. Reprod. Dev. 49, 374–385.

Neuwald, A.F., Aravind, L., Spouge, J.L., Koonin, E.V., 1999. AAA+: a class of chaperone-like ATPases associated with the assembly, operation, and disassembly of protein complexes. Genome Res. 9, 27–43.

Olds-Clarke, P., Johnson, L.R., 1993. *t* haplotypes in the mouse compromise sperm flagellar function. Dev. Biol. 155, 14–25.

Pilder, S.H., Olds-Clarke, P., Phillips, D.M., Silver, L.M., 1993. *Hybrid sterility-6*: a mouse *t* complex locus controlling sperm flagellar assembly and movement. Dev. Biol. 159, 631–642.

Puntervoll, P., Linding, R., Gemund, C., Chabanis-Davidson, S., Mattingsdal, M., Cameron, S., Martin, D.M., Ausiello, G., Brannetti, B., Costantini, A., Ferre, F., Maselli, V., Via, A., Cesareni, G., Diella, F., Superti-Furga, G., Wyrwicz, L., Ramu, C., McGuigan, C., Gudavalli, R., Letunic, I., Bork, P., Rychlewski, L., Kuster, B., Helmer-Citterich, M., Hunter, W.N., Aasland, R., Gibson, T.J., 2003. ELM server: a new resource for investigating short functional sites in modular eukaryotic proteins. Nucleic Acids Res. 31, 3625–3630.

Redkar, A.A., Olds-Clarke, P., Dugan, L.M., Pilder, S.H., 1998. High-resolution mapping of sperm function defects in the *t* complex fourth inversion. Mamm. Genome 9, 825–830.

Ren, D., Navarro, B., Perez, G., Jackson, A.C., Hsu, S., Shi, Q., Tilly, J.L., Clapham, D.E., 2001. A sperm ion channel required for sperm motility and male fertility. Nature 413, 603–609.

Rosenquist, M., Sehnke, P., Ferl, R.J., Sommarin, M., Larsson, C., 2000. Evolution of the 14-3-3 protein family: does the large number of isoforms in multicellular organisms reflect functional specificity? J. Mol. Evol. 51, 446–458.

Rost, B., Liu, J., Nair, R., Wrzeszczynski, K.O., Ofran, Y., 2003. Automatic prediction of protein function. Cell. Mol. Life Sci. 60, 2637–2650.

Samant, S.A., Fossella, J., Silver, L.M., Pilder, S.H., 1999. Mapping and cloning recombinant breakpoints demarcating the *hybrid sterility 6*-specific sperm tail assembly defect. Mamm. Genome 10, 88–94.

Samant, S.A., Ogunkua, O., Hui, L., Fossella, J., Pilder, S.H., 2002. The *t* complex distorter 2 candidate gene, *Dnahc8*, encodes at least two testis-specific axonemal dynein heavy chains that differ extensively at their amino and carboxyl termini. Dev. Biol. 250, 24–43.

Schimenti, J.C., Reynolds, J.L., Planchart, A., 2005. Mutations in Serac1 or Synj2 cause proximal t haplotype-mediated male mouse sterility but not transmission ratio distortion. Proc. Natl. Acad. Sci. U. S. A. 102, 3342–3347.

Schmitz-Lesich, K.A., Lindemann, C.B., 2004. Direct measurement of the passive stiffness of rat sperm and implications to the mechanism of the calcium response. Cell Motil. Cytoskeleton 59, 169–179.

Si, Y., Okuno, M., 1999. Role of tyrosine phosphorylation of flagellar proteins in hamster sperm hyperactivation. Biol. Reprod. 61, 240–246.

Tanaka, Y., Zhang, Z., Hirokawa, N., 1995. Identification and molecular evolution of new dynein-like protein sequences in rat brain. J. Cell Sci. 108, 1883–1893.

Thompson, J.D., Higgins, D.G., Gibson, T.J., 1994. CLUSTAL W: improving the sensitivity of progressive multiple sequence alignment through sequence weighting, position-specific gap penalties and weight matrix choice. Nucleic Acids Res. 22, 4673–4680.

Topham, C.M., McLeod, A., Eisenmenger, F., Overington, J.P., Johnson, M.S., Blundell, T.L., 1993. Fragment ranking in modelling of protein structure. Conformationally constrained environmental amino acid substitution tables. J. Mol. Biol. 229, 194–220.

Vijayaraghavan, S., Liberty, G.A., Mohan, J., Winfrey, V.P., Olson, G.E., Carr, D.W., 1999. Isolation and molecular characterization of AKAP110, a novel, sperm-specific protein kinase A-anchoring protein. Mol. Endocrinol. 13, 705–717.

Williams, R.W., Chang, A., Juretic, D., Loughran, S., 1987. Secondary structure predictions and medium range interactions. Biochim. Biophys. Acta 916, 200–204.

Wu, J., Huang, K.P., Huang, F.L., 2003. Participation of NMDA-mediated phosphorylation and oxidation of neurogranin in the regulation of Ca2+- and Ca2+/calmodulin-dependent neuronal signaling in the hippocampus. J. Neurochem. 86, 1524–1533.

Xang, X.J., 2005. Multisite protein modification and intramolecular signaling. Oncogene 24, 1653–1662.

Yap, K.L., Kim, J., Truong, K., Sherman, M., Yuan, T., Ikura, M., 2000. Calmodulin target database. J. Struct. Funct. Genomics 1, 8–14.

Yoo, J.H., Cheong, M.S., Park, C.Y., Moon, B.C., Kim, M.C., Kang, Y.H., Park, H.C., Choi, M.S., Lee, J.H., Jung, W.Y., Yoon, H.W., Chung, W.S., Lim, C.O., Lee, S.Y., Cho, M.J., 2004. Regulation of the dual specificity protein phosphatase, DsPTP1, through interactions with calmodulin. J. Biol. Chem. 279, 848–858.